

Qubit seriation: Improving data-model alignment using spectral ordering

Atithi Acharya,^{1,2} Manuel Rudolph,¹ Jing Chen,¹ Jacob Miller,¹ and Alejandro Perdomo-Ortiz^{1,*}

¹Zapata Computing Canada Inc., 325 Front St W, Toronto, ON, M5V 2Y1

²Rutgers University, Piscataway, NJ 08854, USA

(Dated: November 30, 2022)

With the advent of quantum and quantum-inspired machine learning, adapting the structure of learning models to match the structure of target datasets has been shown to be crucial for obtaining high performance. Probabilistic models based on tensor networks (TNs) are prime candidates to benefit from data-dependent design considerations, owing to their bias towards correlations which are local with respect to the topology of the model. In this work, we use methods from spectral graph theory to search for optimal permutations of model sites which are adapted to the structure of an input dataset. Our method uses pairwise mutual information estimates from the target dataset to ensure that strongly correlated bits are placed closer to each other relative to the model's topology. We demonstrate the effectiveness of such preprocessing for probabilistic modeling tasks, finding substantial improvements in the performance of generative models based on matrix product states (MPS) across a variety of datasets. We also show how spectral embedding, a dimensionality reduction technique from spectral graph theory, can be used to gain further insights into the structure of datasets of interest.

I. INTRODUCTION

The development of increasingly powerful quantum computers has placed renewed focus on the near-term potential of quantum models and algorithms for solving problems of significant real-world value. Probabilistic modeling, where a model is trained to learn the structure of an unknown distribution from an unlabeled dataset of samples, has emerged as an application of particular promise for quantum methods [1], owing to provable advantages in expressivity [2] and generalization [3] arising from the distinct properties of quantum state spaces. Within this domain, the use of quantum-inspired tensor networks (TNs) has allowed many of the advantages of fully-quantum probabilistic models to be enjoyed in a simulated classical setting [4, 5], while also permitting the development of hybrid quantum-classical models that exploit the complementary properties of both model families for practical benefit [6–9].

Although promising, the relative newness of quantum and quantum-inspired machine learning algorithms means that best practices for ensuring optimal performance remain unsettled. While a large amount of attention has been dedicated to overcoming the phenomenon of *barren plateaus* in optimization landscapes [10–12], we focus here on a less well-understood issue, namely, the impact of the dataset's geometry on the performance of the machine-learning (ML) models. The importance of optimally matching model geometry to the structure of probabilistic modeling problems is well-understood in the TN community [13–15]. However, prior proposals for ensuring this optimal matching have tended to rely on heuristic search through various model configurations [16–18], entailing a high cost due to repeated model retraining, while also failing to make use of insights present in the structure of the classical data itself. A notable exception is the problem-specific solution of Barcza et al. [19], where

spectral ordering methods were shown to be capable of improving the performance of density matrix renormalization group (DMRG) calculations within quantum chemistry problems. Recent efforts to incorporate geometric considerations into quantum machine learning (QML), although of a different flavor than considered here, include the works of [20–23], where the authors incorporate geometric priors arising from problem-specific symmetries into quantum models.

In this work, we introduce a simple method for ordering the variables of a classical dataset to ensure an optimal match between the correlations present in the data and the connectivity of 1D quantum or quantum-inspired models. We refer to this problem as *qubit seriation*, in recognition of its similarity with the seriation problem of linearly-ordering sequential data, which has proven important in domains as diverse as archaeology [24], DNA sequencing [25, 26], and natural language processing [27]. Our approach makes use of tools from spectral graph theory to efficiently compute an ordering directly from the pairwise mutual information between variables in a classical dataset of interest, thus guaranteeing that strongly correlated variables are mapped to nearby qubits, and weakly correlated variables to more distant qubits. We demonstrate the effectiveness of our procedure in probabilistic modeling experiments utilizing matrix product states (MPS), where reordering the variables of a classical dataset prior to optimization is shown to significantly boost the performance of the trained model. We show how spectral embedding tools can be used to extend these methods to models with more complex connectivities, and develop heuristics for understanding the impact of noise or small dataset size on the output ordering. Overall, our work emphasizes the practical importance of geometric considerations in quantum and quantum inspired machine learning, and demonstrates the performance benefits that are possible with the use of principled approaches to solving these issues.

* alejandro@zapatacomputing.com

II. BACKGROUND

A. Spectral Graph Theory and Mutual Information

The central object within spectral graph theory is graph Laplacian matrices. Although there exists several varieties of graph Laplacians, this work will focus on those based on undirected weighted graphs, which are described using a symmetric *weight matrix* $W \in \mathbb{R}^{n \times n}$, whose nonnegative entries $W := (w_{ij})$ specify the edge weights between the n nodes of the corresponding graph. The (unnormalized) graph Laplacian is then given by $L = D - W$, where D is the diagonal *degree matrix* with entries of $D_{ij} = \delta_{ij} \sum_j W_{ij}$. The eigenvalues and eigenvectors of the graph Laplacian can be used to describe and study many properties of their respective graphs [28, 29]. Some important properties of the graph Laplacian include [28]: (1) For every vector $f \in \mathbb{R}^n$ we have

$$f^T L f = \frac{1}{2} \sum_{i,j=1}^n w_{ij} (f_i - f_j)^2. \quad (1)$$

(2) L is symmetric and positive semi-definite. (3) L has n real, non-negative eigenvalues $0 = \lambda_0 \leq \lambda_2 \leq \dots \leq \lambda_{n-1}$, with the (trivial) eigenvector associated with λ_0 being the all-ones vector $\mathbf{x}_0 = \mathbf{1}$. (4) The number of zero eigenvalues $\lambda_i = 0$ is equal to the number of connected components in the graph, such that a graph with k connected components will have λ_k be the first non-zero eigenvector. In the following we will typically assume the use of connected graphs, so that $\lambda_1 > 0$.

The eigenvector associated with the first non-zero eigenvalue is referred to as the *Fiedler vector*, and has a central role in many applications stemming from spectral graph theory. One important application lies in spectral clustering [30] which uses spectral properties of the similarity graph Laplacians. Given a dataset, the goal is to build a similarity graph which models the local neighborhood relationships between the data points. These similarity graphs can be of various kinds such as ϵ -neighborhood graph, k -nearest neighbor graphs, but our work will focus on fully connected graphs. Once a similarity graph is established, the graph Laplacian L can be computed from the corresponding weighted weight matrix W . Then we can directly use the first m eigenvectors stacked as columns in a matrix $U \in \mathbb{R}^{n \times m}$. Performing k -means clustering in this lower-dimensional subspace leads to an effective clustering of the original data points. Beyond spectral clustering, we will utilize the lesser-known formalism of spectral graph ordering III, which will be discussed in Sec. III.

Our work utilizes a similarity graph based on pairwise mutual information, which is simply the mutual information (MI) between each pair of random variables in a distribution. The MI between variables X_i and X_j is defined as $I(X_i; X_j) = D_{\text{KL}}(P_{X_i, X_j} || P_{X_i} P_{X_j})$, where $D_{\text{KL}}(P || Q) = \sum_x P(x) (\log(P(x)) - \log(Q(x)))$ denotes the Kullback-Leibler (KL) divergence. Pairwise MI is not a distance metric between variables in a distribution, and in cases that a proper metric is needed, one can use (for example) a variation of information. The sample complexity for estimating MI is well-

studied in the information theory literature [31], and in the following we employ a maximum likelihood approach to estimate the MI between pairs of variables based on a number of samples from the underlying statistical distribution.

B. Tensor Networks and Born Machines

Tensor networks (TNs) are a family of models for describing large tensors $\psi \in \mathbb{C}^{d_1 \times d_2 \times \dots \times d_n}$ using smaller tensor ‘‘cores’’, which are contracted together in a manner described by a defining graph \mathcal{G} [32]. We focus on the case of matrix product states (MPS), whose n cores $\{\mathcal{A}^{(i)} \in \mathbb{C}^{\chi_{i-1} \times d_i \times \chi_i}\}_{i=1}^n$ are contracted on a line graph along ‘‘bonds’’ of dimension $\chi_i \in \mathbb{N}$, whose size determines the expressivity of the model [33]. Concretely, this describes a tensor with elements given by

$$\psi_{x_1, x_2, \dots, x_n} = \mathcal{A}_{x_1}^{(1)} \mathcal{A}_{x_2}^{(2)} \dots \mathcal{A}_{x_n}^{(n)}, \quad (2)$$

where $\mathcal{A}_{x_i}^{(i)} \in \mathbb{C}^{\chi_{i-1} \times \chi_i}$ denotes the matrix with elements $(\mathcal{A}_{x_i}^{(i)})_{\alpha, \beta} = \mathcal{A}_{\alpha, x_i, \beta}^{(i)}$ and the indices associated with trivial bond dimensions $\chi_0 = \chi_n = 1$ are taken to be $x_0 = x_n = 1$. In the common setting where ψ describes an n -body wavefunction, ψ must be normalized to have unit Frobenius norm, i.e. $\|\psi\|_2^2 = \sum_{x_1, \dots, x_n} |\psi_{x_1, \dots, x_n}|^2 = \sum_{\mathbf{x}} |\psi_{\mathbf{x}}|^2 = 1$, where we use $\mathbf{x} = (x_1, \dots, x_n)$ to denote the collection of all n discrete indices of an MPS, which in our setting will describe the possible values of n discrete variables.

Inspired by their long-established use in simulating many-body quantum systems, MPS have more recently been adapted to the task of learning classical probability distributions [34, 35], where they are referred to as MPS *Born machines* (BMs). Each BM over an n -core MPS defines a probability distribution over n discrete random variables, as $P_{\text{BM}}(\mathbf{x}) = |\psi_{\mathbf{x}}|^2$, which is properly normalized iff $\|\psi\|_2^2 = 1$. The n cores of the MPS are then optimized to minimize a loss function measuring the compatibility of P_{BM} with an unlabeled dataset $\mathcal{D} = \{\mathbf{x}_t\}_{t=1}^T$, which is typically chosen as the negative log likelihood loss $\text{NLL}(P_{\text{BM}}, \mathcal{D})$, defined by

$$\begin{aligned} \text{NLL}(P_{\text{BM}}, \mathcal{D}) &= -\frac{1}{T} \sum_{t=1}^T \ln(P_{\text{BM}}(\mathbf{x}_t)) \\ &= D_{\text{KL}}(P_{\mathcal{D}} || P_{\text{BM}}) + \ln(T), \end{aligned} \quad (3)$$

where $P_{\mathcal{D}}$ is the empirical distribution given by $P_{\mathcal{D}}(\mathbf{x}) = 1/T$ for $\mathbf{x} \in \mathcal{D}$ and $P_{\mathcal{D}}(\mathbf{x}) = 0$ otherwise. Given that $\text{NLL}(P_{\text{BM}}, \mathcal{D})$ is equal to $D_{\text{KL}}(P_{\mathcal{D}} || P_{\text{BM}})$ up to a constant offset, minimizing the former is equivalent to minimizing the latter, which encourages P_{BM} to assign large probability to samples \mathbf{x}_t contained in \mathcal{D} .

Although MPS are ubiquitous in applications of TNs to quantum simulation, machine learning, and other fields, their 1D connectivity leads to a preference for capturing structure associated with sites i, j for which $|i - j|$ is small. The primary reason for this preference is the limited capacity of MPS BMs, where the value of each bond dimension χ_i places an

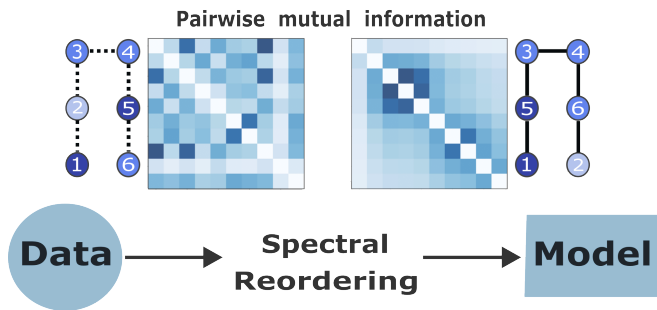


FIG. 1. Schematic representation of our qubit seriation framework: Training data is often not structured such that neighboring sites of data samples are maximally correlated. However our spectral reordering preserves locality, as seen in the pairwise mutual information plots. We can see the unstructured data to the left has correlated qubits farther from each other but after we employ spectral ordering, the pairwise mutual information matrix has larger elements closer to the diagonal, as seen to the right of the figure. This reordering improves the performance of machine learning algorithms, such as those utilizing tensor network models.

upper bound on the achievable MI between random variables associated with sites separated by the corresponding bond. Long-range correlations between two sites must be propagated through all intermediate bonds, which leads to a greater saturation of the capacity of the model than for short-range correlations. At an empirical level, it leads MPS BMs to learning target distributions more rapidly, and with smaller model sizes, when strongly correlated random variables are in close proximity to each other relative to the line graph defining the MPS.

III. METHODS

Qubit seriation using spectral graph ordering

We begin with an outline of a data-driven means of sequentially ordering variables within a distribution, which ensures that more strongly correlated sites are kept closer together than more distant sites. At a high level, this method employs a simple cost function scoring variable permutations based on the extent of long-range correlations in the reordered data. Although optimizing this cost function exactly is likely infeasible, we adopt a spectral ordering solution which uses spectral graph theory [28] to solve a convex relaxation of this original problem. We then develop a concrete connection between qubit seriation and spectral ordering, which makes use of the graph Laplacian associated with pairwise MI statistics in the data.

For data with n sites, the ordering can be defined as the index permutation $\pi(1, 2, \dots, n) = (\pi(1), \pi(2), \dots, \pi(n))$. Each choice of ordering π acts on the weight matrix to give a new matrix $(\pi W \pi^T)_{ij} = w_{\pi(i), \pi(j)}$ expressing the MI between the permuted variables, and we aim to find a choice of π such that larger values $w_{i,j}$ of the original weight matrix are mapped to values $w_{\pi(i), \pi(j)}$ such that $|\pi(i) - \pi(j)|$ is as

small as possible, i.e., larger values in W should be closer to the diagonal. One way of accomplishing this goal is to minimize a permutation-dependent cost function $C_{\text{perm}}(\pi)$, which measures the extent of long-range correlations in the permuted dataset. A straightforward choice of this cost function, which we will see enables the application of useful previous results on spectral ordering, is

$$C_{\text{perm}}(\pi) = \frac{1}{2} \sum_{i,j} (i-j)^2 w_{\pi(i), \pi(j)} \quad (5)$$

While finding the minimum of this cost function is a combinatorial optimization problem which likely cannot be achieved with any polynomial-time algorithm [36], finding a low-cost ordering is nonetheless possible by solving a convex relaxation of this problem. More precisely, the Fiedler vector solves a convex relaxation of C_{perm} in Eq. 5, which is phrased in terms of vectors \mathbf{x} whose entries are continuous variables $x_i \in [-1, 1]$. Additionally, the shifting necessary in the discrete variables introduces a constraint $\sum_i x_i = 0$. The cost function for this convex relaxation is given by

$$C(\mathbf{x}) = \frac{1}{2} \sum_{i,j} (x_i - x_j)^2 w_{i,j} = \mathbf{x}^T L \mathbf{x}, \quad (6)$$

where L denotes the graph Laplacian associated to the matrix of pairwise MI values $w_{i,j}$, and the second equality comes from Eq. 1. See Refs. [25, 26] for a similar analysis in the context of DNA sequencing.

To avoid trivial solutions, this convex relaxation requires the additional constraint $\mathbf{x}^T \mathbf{x} = 1$, which can be imposed using a Lagrange multiplier λ . The stationary points of this cost function occur when \mathbf{x} is an eigenvector of the positive semidefinite operator L . Now the cost function reads as

$$C'(\pi) = \mathbf{x}^T L \mathbf{x} - \lambda(\mathbf{x}^T \mathbf{x} - 1), \quad (7)$$

whose minimization is equivalent to minimizing the Rayleigh quotient $R(x) = \frac{\mathbf{x}^T L \mathbf{x}}{\mathbf{x}^T \mathbf{x}}$. It is straightforward to verify that the minimization of Eq. 7 subject to the constraint $\sum_i x_i = 0$ is accomplished by the Fiedler vector \mathbf{x}_1 .

The solution of Eq. 7, a convex relaxation of Eq. 5, yields a vector \mathbf{x}_1 , but our original goal was to identify an optimal permutation π . The link between these two problems arises by sorting the elements of \mathbf{x}_1 in ascending order, with the resulting permutation giving a heuristic solution to Eq. 5 that is provably optimal for certain families of weighted graphs (see Appendix B for more information). Other ways of relaxing the cost function of Eq. 5 exist and can be exploited for some noisier datasets. One instance of the noise can be attributed to the estimation of the similarity values $w_{i,j}$ from samples. See Appendix A for a brief introduction to the relaxation using doubly stochastic matrices and the paper [25] for more details.

IV. RESULTS

Our spectral ordering method for qubit seriation is experimentally validated in three sections. In Sec. IV A we verify the

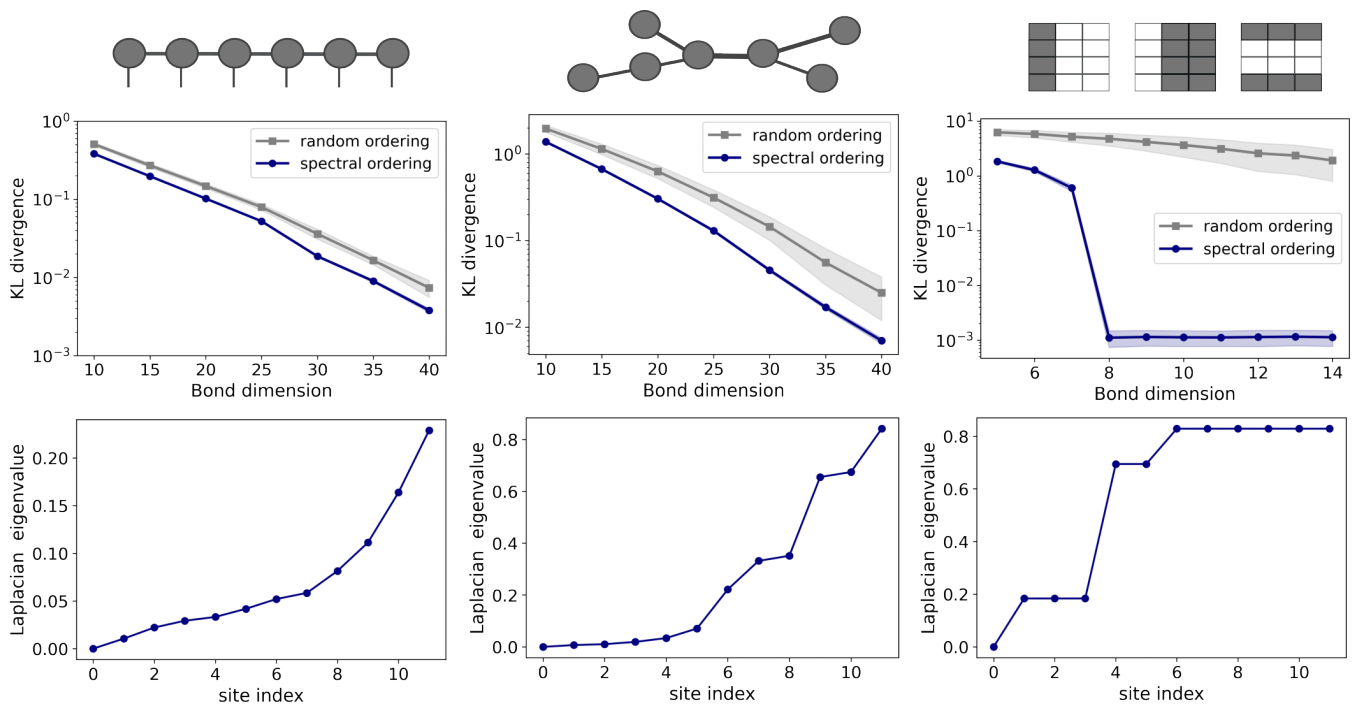


FIG. 2. We plot the final KL divergence between the several training data distributions and trained MPS model distribution using random or seriated feature ordering. We have data generated by a random MPS to the left, followed by samples from a 12-qubit Ising tree Hamiltonian in the center, and finally the 4×3 bars and stripes dataset to the right. The performance of MPS trained using data with random site ordering are marked with gray, while the corresponding results using data with spectral ordering are marked with blue. The gray curves depict the median over 1000 different shufflings of the original dataset, while the fluctuations over these runs are indicated by shaded regions around the plots. In all three cases, the spectral ordering solution leads to a lower training error with greater than (99%) confidence. In the bottom row, we plot the eigenvalues of the corresponding Laplacian.

performance improvement of an MPS-based generative model trained on several datasets when using a spectral ordering of the underlying random variables. In Sec. IV B we then show how higher eigenvectors of the graph Laplacian can be used to reveal additional structural information present in the original dataset. Lastly, in Sec. IV C we analyze the impact of dataset size on the stability of the ordering arising from spectral ordering, which can be assessed using the spectral gap of the graph Laplacian.

A. Spectral ordering based seriation in MPS based models

We demonstrate the success of the solution to qubit seriation with 1D, 2D and other tree-structured data. While training the MPS based generative model using a negative log-likelihood (NLL) loss, we monitor the KL divergence $D_{\text{KL}}(P_{\mathcal{D}}||P_{\text{BM}})$ between the training data distribution $P_{\mathcal{D}}$ and MPS distribution P_{BM} throughout training.

Fig. 2 depicts our numerical simulations on random MPS, the ground states of random tree-structured Ising Hamiltonians, and the bars and stripes (BAS) dataset [35, 37]. Overall, it appears that qubit seriation leads to a better solution in more than 99% of the total 1000 experiments for all three chosen datasets. A final training loss is accepted to be better if it outperforms the randomly-ordered model's loss by more

than a 1% margin. For a study on 1D-correlated datasets, we sampled the distribution associated to random MPS Born machines implemented using the ITensor library [38]. It is worth noting that the improvement for random MPS is not as significant as other datasets. This can likely be attributed to the lack of significant gaps in the spectrum of the graph Laplacian. A similar behavior can be seen in the data collected from the ground state of random tree-structured Ising Hamiltonians:

$$H = - \sum_{i,j} J_{ij} s_i s_j \quad (8)$$

with $s \in \{-1, 1\}$, where importantly, not all J_{ij} are non-zero to retain the tree structure. In this dataset, the seriated MPS show significantly lower KL divergence values, as well as vastly improved variances. Lastly, in the case of the BAS dataset, there are large gaps between the low and the intermediate eigenvalues of the graph Laplacian, indicating that if we use the eigenvector corresponding to a smaller eigenvalue for spectral ordering, we are guaranteed to ensure an ordering that preserves locality. This allows allow the seriated model to closely match the BAS dataset given sufficiently large bond dimensions, while randomly ordered models fail to learn the BAS dataset to any meaningful extent for all bond dimensions investigated.

B. Spectral embedding

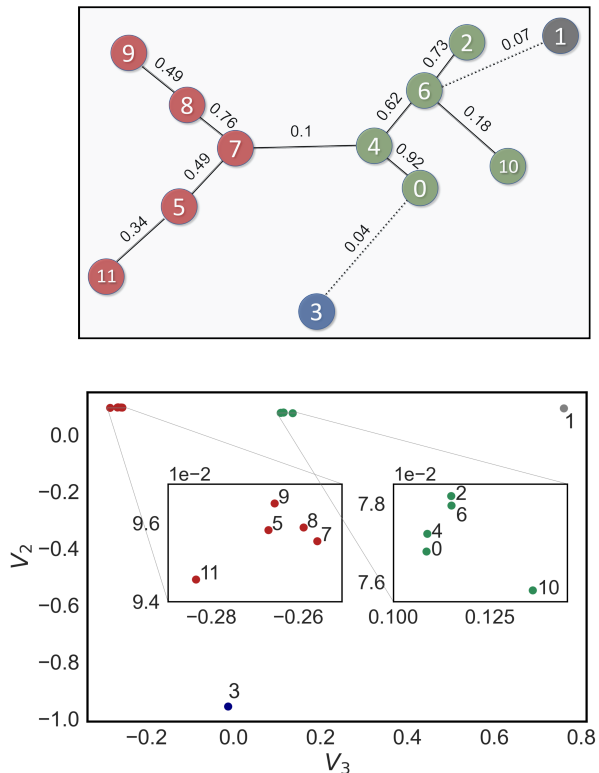


FIG. 3. Demonstrating spectral embedding on an Ising tree dataset. (top): The undirected weighted graph is depicted with weights corresponding to the coupling strength J_{ij} of the Ising Hamiltonian. (bottom): Spectral embedding of the sites in the data using the second and the third eigenvectors of the MI graph Laplacian. We use the MI statistics of 1000 bit-strings corresponding to the ground state configurations of the Ising Hamiltonian on S_z basis. Data sites are colored for convenience. The spectral embedding correctly recovers that qubits numbered [7,8,9,5,11] are clustered separately from [2,6,4,0,10] in terms of their relative correlations. It is important to note that closer distance in the above embedding space indicates stronger correlations between the corresponding variables.

While the Fiedler vector \mathbf{x}_1 encodes the optimal site ordering for 1D correlated data, this may not be optimal for more complicated datasets. In such cases, we can utilize higher eigenvectors of the MI graph Laplacian L . The subspace spanned by these eigenvectors can be used to obtain the so-called spectral embedding. The utility of higher eigenvectors depends on the magnitude of their respective eigenvalues, where the gaps between eigenvalues typically quickly decrease, leading to unstable representations.

As a concrete example, we construct one instance of the Ising tree dataset, given by the ground state of a Hamiltonian described in Eq. (8). The particular tree structure and coefficients J_{ij} can be seen in Fig. 3. Using the spectral embedding on the first two eigenvectors \mathbf{x}_1 and \mathbf{x}_2 , we clearly recover the correlation structure of the ground state which closely follows the magnitude of the J_{ij} terms. We highlight clusters of more closely correlated sites by coloring them in both the Ising tree

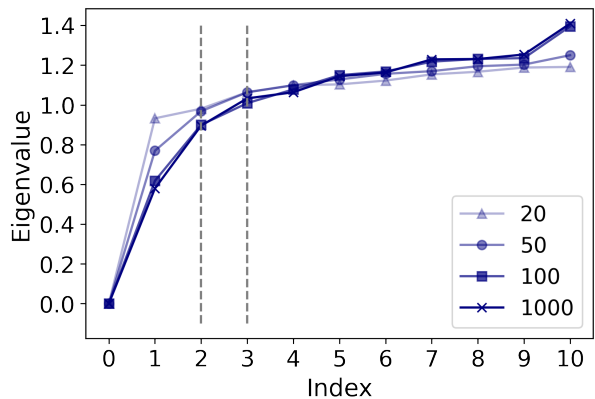


FIG. 4. We see the lessening of spectral gap ($\lambda_1 - \lambda_2$) of the normalized Laplacian if we construct noisier Laplacians by using fewer samples to estimate the pairwise MI matrix. This also means that the Fiedler vector is not a unique vector that will seriate the qubits, meaning that slight variations in the data will generate very different permutations as answers to the seriation problem. The data here is taken from a Markov chain, with the legend showing the number of samples used to estimate the pairwise MI.

graph and the spectral embedding. The embedding can now be utilized to find sparse graphs connecting all sites such that the original full pair-wise MI graph is well-reflected.

C. Stability of the spectral solutions

The stability of the spectral ordering by the Fiedler vector can be indicated by the spectral gap $\lambda_2 - \lambda_1$ of the Laplacian $L(W)$. In general the spectral gap ($\lambda_k - \lambda_{k-1}$) is used for stability analysis when the algorithm uses the subspace formed by k eigenvectors. If there is degeneracy in the system, then there might be more than one optimal solutions since the solutions form a degenerate subspace. It does not matter which direction is picked within the subspace or if a more general algorithm is employed. However, if there is no gap between the bands of eigenvalues, then it is indicative that there will be no benefit to the algorithm via seriation.

The spectral ordering solution is stable when the magnitude of unstructured noise is less than the spectral gap [25].

$$\|\Delta L\|_F \leq (\lambda_k - \lambda_{k-1})/\sqrt{2}$$

Note that this bound is given for an unphysical noise form (see Appendix V). More admissible perturbations that preserve symmetry and non-negativity can be studied but it goes beyond the indication of stability one intends to use from the spectral gap in the methods used in our work. We also demonstrate that the sampling noise in the estimation of MI also leads to the lessening of the spectral gap. Thus further leading to an unstable or less useful solution to seriation (see Fig. 4). Further details can be found in [39], where the authors perform a similar analysis of stability but for closely related spectral clustering problems. We present a proof and interpretation of these results in more detail while also noting the

special cases which lead to stronger guarantees on the spectral solution to seriation.

V. CONCLUSIONS

In our work, we apply spectral graph theory methods for qubit seriation in tensor network based generative models. Given a dataset, we first used an estimate of the pairwise MI between variables to construct a similarity graph Laplacian. We showed how a sorting method based on the lowest non-trivial eigenvector, the Fiedler vector, could be used to improve the performance of trained generative models, which in principle may be either 1D quantum or quantum-inspired algorithms. We further identified how higher non-trivial eigenvectors of the data-dependent graph Laplacian can be used to obtain further insights into the underlying dataset.

While we demonstrated improved training performance us-

ing MPS, other models can also benefit from this. Concretely, clustering algorithms on the spectral embedding of data can be used to design TN architectures and quantum circuit ansätze for ML tasks that are specific to each given dataset. Given that most negative results are derived using uninformed and generic architectures, we are optimistic that our work can lead to improvements in model-data compatibility. We can also leverage the benefits of seriation in generative modeling tasks by classical ML models such as recurrent neural networks and its variants, using the fact that sequential learning is sensitive to data ordering [27].

ACKNOWLEDGMENTS

The authors would like to acknowledge Mohamed Hibat-Allah, Vladimir Vargas-Calderón, and Anirvan Sengupta for their insightful discussions.

-
- [1] Alejandro Perdomo-Ortiz, Marcello Benedetti, John Realpe-Gómez, and Rupak Biswas, “Opportunities and challenges for quantum-assisted machine learning in near-term quantum computers,” *Quantum Science and Technology* **3**, 030502 (2018).
 - [2] Xun Gao, Eric R. Anschuetz, Sheng-Tao Wang, J. Ignacio Cirac, and Mikhail D. Lukin, “Enhancing generative models via quantum correlations,” *Phys. Rev. X* **12**, 021037 (2022).
 - [3] Kaitlin Gili, Marta Mauri, and Alejandro Perdomo-Ortiz, “Evaluating generalization in classical and quantum generative models,” arXiv:2201.08770 (2022).
 - [4] Ivan Glasser, Ryan Sweke, Nicola Pancotti, Jens Eisert, and Ignacio Cirac, “Expressive power of tensor-network factorizations for probabilistic modeling,” *Advances in neural information processing systems* **32** (2019).
 - [5] Tai-Danae Bradley, E M Stoudenmire, and John Terilla, “Modeling sequences with quantum states: a look under the hood,” *Machine Learning: Science and Technology* **1**, 035008 (2020).
 - [6] Xun Gao, Zhengyu Zhang, and Luming Duan, “A quantum machine learning algorithm based on generative models,” *Science Advances* **4** (2018), 10.1126/sciadv.aat9004.
 - [7] William Huggins, Piyush Patil, Bradley Mitchell, K Birgitta Whaley, and E Miles Stoudenmire, “Towards quantum machine learning with tensor networks,” *Quantum Science and Technology* **4**, 024001 (2019).
 - [8] Michael L Wall, Matthew R Abernathy, and Gregory Quiroz, “Generative machine learning with tensor networks: Benchmarks on near-term quantum computers,” *Physical Review Research* **3**, 023010 (2021).
 - [9] Manuel S. Rudolph, Jacob Miller, Jing Chen, Atithi Acharya, and Alejandro Perdomo-Ortiz, “Synergy between quantum circuits and tensor networks: Short-cutting the race to practical quantum advantage,” arXiv preprint arXiv:2208.13673 (2022).
 - [10] Jarrod McClean, Sergio Boixo, Vadim Smelyanskiy, Ryan Babush, and Hartmut Neven, “Barren plateaus in quantum neural network training landscapes,” *Nature Communications* **9** (2018).
 - [11] Marco Cerezo, Akira Sone, Tyler Volkoff, Lukasz Cincio, and Patrick J Coles, “Cost function dependent barren plateaus in shallow parametrized quantum circuits,” *Nature communications* **12**, 1–12 (2021).
 - [12] Zoë Holmes, Kunal Sharma, Marco Cerezo, and Patrick J Coles, “Connecting ansatz expressibility to gradient magnitudes and barren plateaus,” *PRX Quantum* **3**, 010313 (2022).
 - [13] Glen Evenbly and Guifré Vidal, “Tensor network states and geometry,” *Journal of Statistical Physics* **145**, 891–918 (2011).
 - [14] Sirui Lu, Márton Kanász-Nagy, Ivan Kukuljan, and J Ignacio Cirac, “Tensor networks and efficient descriptions of classical data,” arXiv preprint arXiv:2103.06872 (2021).
 - [15] Ian Convy, William Huggins, Haoran Liao, and K Birgitta Whaley, “Mutual information scaling for tensor network machine learning,” *Machine learning: science and technology* **3**, 015017 (2022).
 - [16] Chao Li and Zhun Sun, “Evolutionary topology search for tensor network decomposition,” in *International Conference on Machine Learning* (PMLR, 2020) pp. 5947–5957.
 - [17] Meraj Hashemizadeh, Michelle Liu, Jacob Miller, and Guillaume Rabusseau, “Adaptive learning of tensor network structures,” arXiv preprint arXiv:2008.05437 (2020).
 - [18] Chao Li, Junhua Zeng, Zerui Tao, and Qibin Zhao, “Permutation search of tensor network structures via local sampling,” in *International Conference on Machine Learning* (PMLR, 2022) pp. 13106–13124.
 - [19] G. Barcza, Ö. Legeza, K. H. Marti, and M. Reiher, “Quantum-information analysis of electronic states of different molecular structures,” *Physical Review A* **83** (2011), 10.1103/physreva.83.012508.
 - [20] Johannes Jakob Meyer, Marian Mularski, Elies Gil-Fuster, Antonio Anna Mele, Francesco Arzani, Alissa Wilms, and Jens Eisert, “Exploiting symmetry in variational quantum machine learning,” arXiv preprint arXiv:2205.06217 (2022).
 - [21] Martín Larocca, Frédéric Sauvage, Faris M. Sbahi, Guillaume Verdon, Patrick J. Coles, and M. Cerezo, “Group-invariant quantum machine learning,” *PRX Quantum* **3** (2022), 10.1103/prxquantum.3.030341.
 - [22] Michael Ragone, Paolo Braccia, Quynh T Nguyen, Louis Schatzki, Patrick J Coles, Frederic Sauvage, Martin Larocca, and M Cerezo, “Representation theory for geometric quantum machine learning,” arXiv preprint arXiv:2210.07980 (2022).
 - [23] Quynh T Nguyen, Louis Schatzki, Paolo Braccia, Michael Ragone, Patrick J Coles, Frederic Sauvage, Martin Larocca,

- and M Cerezo, “Theory for equivariant quantum neural networks,” arXiv preprint arXiv:2210.08566 (2022).
- [24] W. S. Robinson, “A method for chronologically ordering archaeological deposits,” *American Antiquity* **16**, 293–301 (1951).
- [25] Fajwel Fogel, Rodolphe Jenatton, Francis Bach, and Alexandre d’Aspremont, “Convex relaxations for permutation problems,” (2013).
- [26] Jonathan E. Atkins, Erik G. Boman, and Bruce Hendrickson, “A spectral algorithm for seriation and the consecutive ones problem,” *SIAM Journal on Computing* **28**, 297–310 (1998), <https://doi.org/10.1137/S0097539795285771>.
- [27] Oriol Vinyals, Samy Bengio, and Manjunath Kudlur, “Order matters: Sequence to sequence for sets,” (2015).
- [28] Ulrike Von Luxburg, “A tutorial on spectral clustering,” *Statistics and computing* **17**, 395–416 (2007).
- [29] Bojan Mohar, “Some applications of laplace eigenvalues of graphs,” in *Graph Symmetry: Algebraic Methods and Applications*, edited by Geña Hahn and Gert Sabidussi (Springer Netherlands, Dordrecht, 1997) pp. 225–275.
- [30] Andrew Ng, Michael Jordan, and Yair Weiss, “On spectral clustering: Analysis and an algorithm,” in *Advances in Neural Information Processing Systems*, Vol. 14, edited by T. Dietterich, S. Becker, and Z. Ghahramani (MIT Press, 2001).
- [31] Liam Paninski, “Estimation of entropy and mutual information,” *Neural Comput.* **15**, 1191–1253 (2003).
- [32] Román Orús, “A practical introduction to tensor networks: Matrix product states and projected entangled pair states,” *Annals of physics* **349**, 117–158 (2014).
- [33] D Perez-Garcia, F Verstraete, MM Wolf, and JI Cirac, “Matrix product state representations,” *Quantum Information & Computation* **7**, 401–430 (2007).
- [34] Andrew J Ferris and Guifre Vidal, “Perfect sampling with unitary tensor networks,” *Physical Review B* **85**, 165146 (2012).
- [35] Zhao-Yu Han, Jun Wang, Heng Fan, Lei Wang, and Pan Zhang, “Unsupervised generative modeling using matrix product states,” *PRX* **8**, 031012 (2018).
- [36] Chris Ding and Xiaofeng He, “Linearized cluster assignment via spectral ordering,” in *Proceedings of the twenty-first international conference on Machine learning* (2004) p. 30.
- [37] Marcello Benedetti, Delfina Garcia-Pintos, Yunseong Nam, and Alejandro Perdomo-Ortiz, “A generative modeling approach for benchmarking and training shallow quantum circuits,” *npj Quantum Information* **5** (2018), 10.1038/s41534-019-0157-8.
- [38] Matthew Fishman, Steven R. White, and E. Miles Stoudenmire, “The itensor software library for tensor network calculations,” (2020).
- [39] Eleonora Andreotti, Dominik Edelmann, Nicola Guglielmi, and Christian Lubich, “Measuring the stability of spectral clustering,” (2019).
- [40] Ying Liu, “Preliminary study of connectivity for quantum key distribution network,” (2020).

Appendix A: Spectral ordering

We are trying to insure that after the data has been ordered, the adjacent qubits are similar where as the distant qubits are less similar. The ordering can be defined as the index permutation $\pi(1, 2, \dots, n) = (\pi(1), \pi(2), \dots, \pi(n))$. The permuted mutual information matrix is $(\pi W \pi^T)_{ij} = w_{\pi(i), \pi(j)}$.

The cost function can then be written as $C(\pi) = \frac{1}{2} \sum_{i,j} (i-j)^2 w_{\pi(i), \pi(j)}$. Using the permutation substitution i.e. $i \rightarrow \pi^{-1}(i)$ which results in the replacement $\pi(i) \rightarrow i$, we get the expression

$$C(\pi) = \frac{1}{2} \sum_{i,j} (\pi^{-1}(i) - \pi^{-1}(j))^2 w_{i,j}$$

To further simplify the cost function, one can shift the terms as follows. $(\pi^{-1}(i) - c - (\pi^{-1}(j) - c))^2$. Since $\sum_i \pi(i) = \frac{n(n+1)}{2}$, we can use $cn = \frac{n(n+1)}{2} \implies c = \frac{(n+1)}{2}$.

$$C(\pi) = \frac{n^2}{8} \sum_{i,j} (x_i - x_j)^2 w_{i,j}$$

$$x_i = \frac{\pi^{-1}(i) - (n+1)/2}{n/2} \quad \text{s.t.} \quad \sum_i x_i = 0$$

We can finally rescale the terms since it doesn’t change anything to our optimal solution i.e. the permutations. After scaling appropriately, we can enforce an additional condition on the scaled x in order for it to satisfy $\mathbf{x}^T \mathbf{x} = \sum_i x_i^2 = 1$. Note that, so far we are trying to find the optimal solution for the discrete values of \mathbf{x} and it is in fact a combinatorial optimization problem known to be hard [36]. The new cost function in terms of the rescaled and shifted variables which we still call x can be written as

$$C(\pi) = \frac{1}{2} \sum_{i,j} (x_i - x_j)^2 w_{i,j}$$

$$\text{s.t.} \quad \sum_i x_i = 0, \quad \sum_i x_i^2 = 1$$

Where the possibilities of x_i are still discrete and come from a scaled version of $\frac{\pi^{-1}(i) - (n+1)/2}{n/2}$. However, we can secretly invoke the quadratic laplacian form by following the steps below.

$$C(\pi) = \frac{1}{2} \sum_{i,j} (x_i^2 + x_j^2 - 2x_i x_j) w_{i,j} \tag{A1}$$

$$= \frac{1}{2} \left(\sum_i x_i^2 \sum_j w_{i,j} - 2 \sum_{i,j} x_i x_j w_{i,j} + \sum_j x_j^2 \sum_i w_{i,j} \right) \tag{A2}$$

$$= \frac{1}{2} \left(2 \sum_i x_i^2 \sum_j w_{i,j} - 2 \sum_{i,j} x_i x_j w_{i,j} \right) \tag{A3}$$

$$= \left(\sum_i x_i^2 d_i - \sum_{i,j} x_i x_j w_{i,j} \right) \tag{A4}$$

$$= \mathbf{x}^T (D - W) \mathbf{x} \tag{A5}$$

We used the definition of the Degree matrix $D = \text{diag}(\{d_i\})$ i.e. $d_i = \sum_j W_{ij}$ where W can be read as the adjacency matrix leading to the graph laplacian $L = D - W$. Since the

problem is still discrete, minimizing this along with the constraint that $\sum_i x_i$ while maintaining $\sum_i x_i = 0$ is hard. However, we can relax this condition by letting x_i be continuous and $x_i \in [-1, 1]$. See [25], [26] for a similar analysis that was intended for applications in DNA sequencing. We can add a lagrange multiplier for the second condition i.e. $\mathbf{x}^T \mathbf{x} = 1$. The cost function reads as

$$C(\pi) = \mathbf{x}^T L \mathbf{x} - \lambda(\mathbf{x}^T \mathbf{x} - 1)$$

This is identical to writing the Rayleigh quotient for L and \mathbf{x} and then minimizing it. $R(L, \mathbf{x}) = \frac{\mathbf{x}^T L \mathbf{x}}{\mathbf{x}^T \mathbf{x}}$, and the stationary points of this cost function occurs when \mathbf{x} is the eigenvector of the positive semidefinite operator L . Hence optimality is when $L \mathbf{x} = \lambda \mathbf{x}$ and $R(L, \mathbf{x}) = \lambda$. The lowest eigenvalue of the laplacian is always $\lambda_{min} = 0$ with the eigenvector being the $\mathbf{x}_0 = (1, 1, \dots, 1)^T$. Since L is positive semi-definite, we have $\lambda_{n-1} \geq \lambda_{n-2} \geq \lambda_{n-3} \dots \geq \lambda_0$. The next $n-1$ eigenvectors are orthogonal to \mathbf{x}_0 which then satisfied the $\sum_i x_i = 0$ condition trivially as it can be read as $\mathbf{x}^T \mathbf{x}_0 = 0$. This helps us in identifying that the \mathbf{x}_1 minimizes the cost function while maintaining the constraints. And the n components of the second smallest eigenvector of the graph Laplacian will provide us with the permutations needed to order the qubits respecting the condition that nearby qubits will have more similarity [28].

There are alternative convex relaxation techniques which are useful to provide stable solutions with specific datasets. It uses \mathcal{S}_n the set of doubly stochastic matrices, i.e. $\mathcal{S}_n = \{X \in \mathbb{R}^{n \times n} : X \geq 0, X \mathbf{1} = \mathbf{1}, X^T \mathbf{1} = \mathbf{1}\}$ which is the convex hull of the set of permutation matrices. We can recover the permutation matrix by imposing orthogonality conditions $\Pi = \mathcal{S} \cap \mathcal{O}$, i.e. a matrix is a permutation matrix if and only if it is both doubly stochastic and orthogonal. The fact that $L_A \succeq 0$ means that we can directly write a convex relaxation to the combinatorial problem (5) by replacing \diamond with its convex hull \mathcal{S}_n , to get

$$\begin{aligned} & \text{minimize } g^T X^T L_A X g \\ & \text{subject to } X \mathbf{1} = \mathbf{1}, X^T \mathbf{1} = \mathbf{1}, X \geq 0, \end{aligned} \quad (\text{A6})$$

where $g = (1, \dots, n)$, in the permutation matrix variable $X \in \Pi$. By symmetry, if a vector Xy minimizes (A6), then the reverse vector also minimizes (A6). Since this has a significant negative impact on the quality of the relaxation, the authors [25] added the linear constraint $e_1^T X g + 1 \leq e_n^T X g$ to break symmetries, which means that solutions where the first element comes before the last one is always picked.

Appendix B: Stability of spectral solution

Exact solution: If the underlying similarity matrix is a pre-R matrix (named after W.S. Robinson [24] who defined the property of these matrices, then spectral ordering can be used [26]. A matrix is a R-matrix if it satisfies a simple condition stating that $w_{i,j} \leq w_{i,k}$ for $j < k < i$ and $w_{i,j} \geq w_{i,k}$ for $i < j < k$. The mutual information matrix will be a pre-R matrix iff there exist a permutation π such that $\pi W \pi^T$ is a R matrix. The coefficients of W decrease as we move away from

the diagonal. This basically leads to a guaranteed monotonic Fiedler vector. [26]

Low noise and inside perturbation regime: We also discuss the stability of solutions where the underlying matrix does not have the above properties. The spectral ordering solution can be shown to be stable when there is a significant spectral gap. Further understanding of this is supported by the following analysis where we begin by diagonalizing $L = O \Lambda O^T$, where $\Lambda = \text{diag}(\lambda_i)$ and the orthogonal matrix O constitutes eigenvectors. Let us construct $L_{in} = O \Lambda_{in} O^T$ where “in” is short for interpolated. While all the eigenvalues are the same except for $\lambda_k = \lambda_{k+1} = \frac{1}{2}(\lambda_k + \lambda_{k+1})$, e.g. $\lambda_2 = \lambda_3 = \frac{1}{2}(\lambda_2 + \lambda_3)$. This is how the algorithm can fail to generate stable solution, since two different directions (associated with the eigenvectors of the Laplacian) can now minimize the ordering objective function: If the system is actually degenerate, then we will have to take the degenerate subspace. It doesn’t matter which direction is picked within the subspace or if a more general algorithm is employed. However, if there is no gap between the bands of eigenvalues, then it will in many cases lead to the application not bringing any advantage. Since the cost function Eq. (6) isn’t getting lowered by the spectral solutions.

$$\|L - L_{in}\|_F^2 = \|\Lambda - \Lambda_{in}\|_F^2 = \frac{1}{2}(\lambda_3 - \lambda_2)^2. \quad (\text{B1})$$

$\|\cdot\|_F = \sqrt{\sum_{i,j} l_{i,j}^2}$ denotes the Frobenius norm. The final piece of the puzzle lies in taking an arbitrary matrix \hat{L} with ordered eigenvalues with $\hat{\lambda}_2 = \hat{\lambda}_3$. $\frac{1}{2}(\lambda_2 - \lambda_3)^2 = \min_{\lambda} ((\lambda_2 - \lambda)^2 + (\lambda_3 - \lambda)^2) \leq ((\lambda_2 - \hat{\lambda})^2 + (\lambda_3 - \hat{\lambda})^2)$. Here, we can use the Hoffman-Wielandt theorem to show $\sum_i (\lambda_i - \hat{\lambda}_i)^2 \leq \|L - \hat{L}\|_F^2$ and thus finally we get

$$\frac{1}{2}(\lambda_3 - \lambda_2)^2 \leq \|L - \hat{L}\|_F^2. \quad (\text{B2})$$

It is useful to work out the sketch of proof of the Hoffman-Wielandt theorem as it has hints towards using more noise robust algorithms for the ordering problem.

Since symmetric matrices are diagonalizable by orthogonal matrices, we can write $L = O \Lambda O^T$ and $\hat{L} = U \Sigma U^T$ with $O O^T = U U^T = \mathbf{I}$.

Frobenius norm for symmetric matrices simplifies as $\|A\|_F^2 = \text{Tr}(A A^T) = \text{Tr}(A^2)$. The theorem can be written as the following inequation.

$$\text{Tr}((\Lambda - \Sigma)(\Lambda - \Sigma)^T) \leq \|L - \hat{L}\|_F^2 \quad (\text{B3})$$

$$\text{Tr}((\Lambda - \Sigma)^2) \leq \text{Tr}((O \Lambda O^T - U \Sigma U^T)^2) \quad (\text{B4})$$

Expanding the square leads to elimination of terms, and we are left to show $\text{Tr}(\Lambda O^T U \Sigma U^T O) \leq \text{Tr}(\Lambda \Sigma)$. We can introduce a shorthand $X = O^T U$ to show this. The brute force approach is to maximize $\text{Tr}(\Lambda X \Sigma X^T)$ with the orthogonality constraint $X X^T = \mathbf{I}$. We can use lagrange multiplier Λ_l (a matrix here), to write the objective as

$$C = \text{Tr}(\Lambda X \Sigma X^T) - \text{Tr}(\Lambda_l (X X^T - \mathbf{I})) \quad (\text{B5})$$

While $\frac{\partial C}{\partial \Lambda_l}$ yields the orthogonality constraint. Setting $\frac{\partial C}{\partial X} = 0$ reveals more.

$$\frac{\partial C}{\partial X} = 2\Lambda X \Sigma - (\Lambda_l + \Lambda_l^T)X = 0$$

Since $\text{Tr}(\Lambda_l X X^T) = \text{Tr}(\Lambda_l^T X X^T)$, we can use $\frac{\partial C}{\partial X} = 0$ to find the optimal value of C i.e. $\tilde{C} = \text{Tr}(\Lambda X \Sigma X^T) - \frac{1}{2} \text{Tr}((\Lambda_l + \Lambda_l^T)(X X^T - \mathbf{1})) = \frac{1}{2} \text{Tr}(\Lambda_l + \Lambda_l^T)$.

Appendix C: Algebraic connectivity

Algebraic connectivity has been used to indicate the transmission throughput of a grid quantum network [40]. However, there is also a connection that can be seen between the algebraic connectivity of the graph Laplacian constructed using mutual information as a similarity measure between distributions lying on qubits with the amount of entanglement present in the quantum state. As a numerical experiment, we show the relationship with algebraic connectivity and the bond dimension in a random matrix product state. As the bond dimension increases, indicating a higher entanglement strength, unsurprisingly, we do get the λ_2 to increase as well. We compute

the spectrum and the second smallest eigenvector of the normalized laplacian $D^{-\frac{1}{2}} L D^{-\frac{1}{2}}$.

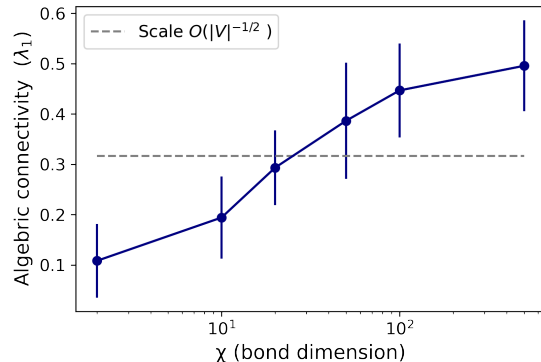


FIG. 5. Algebraic connectivity (the first non-zero eigenvalue) against increasing bond dimension. Here, we take 1000 samples from random MPS with varied bond dimension, estimate pairwise mutual information and then plot the second eigenvalue of the graph laplacian. This indicates that the connectivity increases with increase of entanglement in the quantum state.

We can better understand the behaviour of the connectivity of the graphs formed out of 2-point mutual information by monitoring it for varied amount of noise strengths.